Molecular gas and dust around a radio-quiet quasar at redshift 4.7

Alain Omont [1], Patrick Petitjean [1,2], Stéphane Guilloteau [3]

Richard G. McMahon [4], P. M. Solomon [5], Emmanuel Pécontal [6]

[1] Institut d'Astrophysique de Paris–CNRS, 98bis Bd Arago, F–75014 Paris, France.

[2] DAEC, URA CNRS 173, Observatoire de Paris-Meudon, F-92195 Meudon, France.

[3] Institut de Radio Astronomie Millimétrique, F–38460 St Martin d'Hères, France.

[4] Institute of Astronomy, Madingley Road, Cambridge CB3 0HA, UK.

[5] Astronomy Program, State University of New York, Stony Brook, NY 11794–2100, USA.

[6] Centre de Recherche Astronomique de Lyon, CNRS UMR 142, 9 Avenue Charles André, F–69561, St Genis Laval, France.

email: omont,petitjean@iap.fr, guillote@iram.fr, rgm@ast.cam,ac.uk, psolomon@sbastk.ess.sunysb.edu, pecontal@obs.univ-lyon1.fr

arXiv:astro-ph/9608006v1 1 Aug 1996

Galaxies are believed to form a large proportion of their stars in giant bursts of star formation early in their lives, but when and how this took place are still very uncertain. The presence of very large amounts of dust in objects at the largest known redshifts, quasars and radiogalaxies at z≥4[1–6] shows that some syhthesis of heavy elements has already occurred at this time. This implies that molecular gas–the building material of stars– should also be present as it is in galaxies at lower redshifts[7–10]. Here we report the detection of emission from dust and carbon monoxide in the radio-quiet quasar BR1202–0725 at redshift z=4.7. Maps of these emissions reveal two objects separated by a few arc seconds, which could indicate either the presence of a companion to the quasar or gravitational lensing of the quasar itself. Regardless of the precise interpretation of the maps, the detection of carbon monoxide confirms the presence of a large mass of molecular gas in one of the most distant galaxies known, and shows that conditions conducive to the huge bursts of star formation existed in the very early Universe.

We used the 4 15m-antenna interferometer of the Institut de Radio Astronomie Millimétrique (IRAM) on the Plateau de Bure, France, in Dec. 1995 and Jan. 1996, for a total integration time of ∼ 16 hours with projected baselines from 15m to 160m. Simultaneous measurements were made at $\lambda = 1.35$ and 2.9mm for the purpose of measuring the dust continuum and the CO(5-4) line respectively. The redshift coverage, centered at the approximate redshift of the Lyα line of the companion[12], is 4.679 to 4.730 for the CO(5-4) line (velocity range 2700 km/s). The equivalent single band system temperatures were ∼120–150K and ∼300K at 3mm and 1.35mm respectively. Additional data was obtained in Apr. 1996 at $\lambda = 1.35$mm, and at 3.7mm to measure the CO(4-3) line over redshift range 4.675 to 4.709.

The 1.35mm continuum emission consists in an elongated source at the position of the

quasar, and a second component about 4" to the North-West with ~35% of the total flux. Fig. 1 displays the various features detected in the visible superposed on the millimetre map. The coincidence of the visible position Q of the quasar with the main millimetre peak is almost perfect and well within the uncertainty, $\sim 0.5''$, of the relative position of the quasar with respect to the millimetre map frame. The millimetre emission is extended in the NW direction where a companion to the quasar has been detected in the optical and near–infrared broad-band images[11−14] However, it is seen in Fig. 1 that there is definitely no coincidence between these companion visible features and the NW 1.35mm peak.

Spectra in the redshift range 4.679-4.704 of the CO(5–4) line, with a velocity resolution of 60 km.s^{-1}, are shown in Fig. 2 at various positions. Line emission is detected towards both sources, with an integrated intensity of 1.1± 0.2 Jy.km.s^{-1} towards the quasar and 1.3 ± 0.3 Jy.km.s^{-1} towards the NW peak. However, the actual linewidth is uncertain in the latter position. No signal is detected at other positions in the map (Fig. 1d, 1e and 2). The displayed fits yield a FWHM=190 km/s and a central z=4.6947 at Q, and 350 km/s and z=4.6916 at NW. The derived widths are in the range observed for other high redshift sources: 220 km/s for F10214+4724[9], 326 km/s in H1413+117[10], from 150 to 550 km/s for a sample of 37 ultraluminous galaxies[7,15].

Each of these lines is detected at $\simeq 5 - 6\sigma$ level. Since both detections are independent because the two positions are spatially resolved, CO(5-4) emission is definitely detected at about the 8σ level. The coincidences with the two 1.35mm peak positions and the absence of signal elsewhere (Fig. 1de) further strengthen this conclusion. The lack of pure continuum emission when all the 3mm broad band measurements, except in the line frequency range, are included indicates the detected 3mm emission comes from a spectral line (Fig. 1b).

The presence of CO is further confirmed by the detection of other lines. The 3.7 mm J=4-3 line is detected at the 5-6σ level with integrated flux 1.5±0.3 Jy km s^{-1} (see Fig 1e). No

continuum was detected at this frequency (Fig 1c).

Moreover, the CO(7-6) line (Fig. 2) is present at the 3σ level in a spectrum taken in November 1993 with the IRAM 30m telescope at Pico Veleta Spain. Its integrated flux (3.1 ± 0.86 Jy km s^{-1}), central redshift ($4.6915 \pm.001$) and width ($\sim$250–300 km/s) are consistent with the 5–4 line detected at Bure, taking into account the large 2mm beam of the 30m ($17''$) and excitation conditions similar to F10214+4724[9] and H1413+117[16]. The observed flux ratio $= 3.1/2.4$ translates into a brightness temperature (or line luminosity, L') ratio for the (7-6)/(5-4) lines of 0.65 indicating warm gas. In order to estimate the mass of molecular hydrogen in BR1202$-$0725, several approximations are required. The high rotational temperature inferred from the above ratio indicates that the line luminosity L' will not be much larger for lower J levels. Thus, using the (5-4) line luminosity and a conversion factor $M(H_2)/L'_{CO} = 4$ (see ref 9), we obtain $M(H_2) = 6 \times 10^{10} M_\odot$. This is probably an overestimate; the H$_2$ mass derived this way for ultraluminous IR galaxies with similar CO luminosities[7,15] is too high by about a factor of 3.

Another high redshift object with similar apparent dust and gas properties is F10214+4724 at z = 2.3, a lensed infrared galaxy. Table 1 details the comparison of the emission from BR1202$-$0725 and F10214+4724. It is seen that the observed 3mm integrated line flux and luminosity as well as the apparent molecular mass, are only a factor $\sim$2 smaller in BR1202$-$0725. The actual luminosity and H$_2$ mass depend on an eventual magnification (see below). The relative strengths of the rest frame far infrared/submm and CO emissions, after applying a K (redshift) correction for the dust spectrum are strikingly similar in BR1202$-$0725 and F10214+4724[9], and also in H1413+117 (Cloverleaf)[10,17].

At z=4.7, the $\sim 4''$ mm extension typically corresponds to a projected distance of $\sim$12–30 kpc. If there is no strong lensing, there are at least two distinct far–infrared emitters with their own heating source (AGN and/or starburst). The mass of dust, given

by Eq 1 in ref [1], should be comparable in both sources and $\sim 10^8$ M$_\odot$. These two nearby relatively massive galaxies may thus have formed simultaneously, probably in an early stage of the formation of the central core of a cluster, and they could rapidly merge in a time comparable to the time scale of the activity of bright quasars ($\sim 10^8$ yr, see e.g. [19]). The companion observed in the millimetre continuum could be similar to F10214+4724, with most of its energy emitted in the far infrared. However, contrary to F10214+4724, it is not detected in the visible. The strong tidal interaction between both objects can boost both the star-formation and AGN activity. It is worth noting that the companion, has a CO redshift z=4.6915, FWHM=250-300 km/s, very close (with a difference in velocity of ~ 200 km/s) to that of the metallic absorption system at z=4.688[20] (FWHM = 260 km/s [20]). The absorption system may be due to the halo of the millimetre galaxy companion.

The possibility that the double image is due to gravitational lensing should also be considered. Lensing effects are clear on optical images of the other high redhsift QSO's with CO emission, H1413+117 (Cloverleaf, 4 images[22]) and F10214+4724 (gravitational arc system, see e.g.[21,22] and references therein). Optical amplification factors of ~ 10 or larger are inferred and for F10214+4724 the magnification of the CO emission is of the order of 5–10[25,]. The Cloverleaf also clearly shows evidence of lensing in the CO emission[24]. There are some indications of the possibility of strong lensing on the line of sight to BR1202−0725; B. Fort and S. D'Odorico (private communication) have measured a strong gravitational shear in the field. The line of sight to BR1202−0725 itself has strong absorption systems at z=1.75, 2.44 and 4.38 [19,25,26]. A good explanation of the absence of the second bright optical image could be a strong interstellar absorption in the deflector galaxy along one light path only. Such cases of strong absorption in lens systems are known (see e.g. ref [27]). However, the faint Lyα companion is unlikely to be the result of lensing since it has a spectral energy distribution[11−14] and emission line spectrum different from that of the quasar.

In either case, no lensing or modest magnification of the CO emission, these observations clearly show, for the first time, the presence of a large mass of molecular gas and dust in one of the most distant – and hence youngest – quasars. Combined with the other detections of CO in quasars at z $\approx$ 2.5, this seems to settle completely the question of whether high-redshift quasars are associated with galaxies. BR1202−0725 has a CO luminosity comparable to the highest observed in nearby luminous IR galaxies[7,15], which show characteristics of huge starbursts and AGN's. Thus, star formation in a massive metal enriched ISM, existed very early in the history of the Universe only 0.7 Gyr after the Big Bang ($H_0 = 75$, $q_0 = 0.5$). This supports the idea that the emergence of quasars at very high redshift is connected with the onset of galaxy formation, possibly with formation of the core of ellipticals (see e.g. ref [32]), although nearby quasars also show strong CO emission.

The companion of BR1202−0725, if real, may be an infrared galaxy with very high extinction in the optical and ultraviolet. If the companion is representative of young galaxies, massive star formation at very high redshift will be visible primarily at millimeter wavelengths.

1. McMahon, R.G., Omont, A., Bergeron, J., Kreysa, E., Haslam, C.G.T., *MNRAS*, **267**, L9-L12 (1994)

2. Isaak, K.G., McMahon, R.G., Hills, R.E., Withington,S., *MNRAS*, **269**, L28-L32 (1994)

3. Dunlop, J.S., Hughes, D.H., Rawlings, S., Eales, S., Ward, M., *Nature*, **370**, 347-349 (1994)

4. Chini, R., Krügel, E., *Astron. Astrophys.*, **288**, L33-L36 (1994)

5. Ivison, R.J., *MNRAS*, **275**, L33-L36 (1995)

6. Omont, A., McMahon, R.G., Cox, P., Kreysa, E., Bergeron, J., Pajot, F. and Storrie-Lombardi, L.J., *Astron. Astrophys.* in press (1996)

7. Solomon, P.M., Downes, D., Radford, S.J.E., and Barret, J.W., *Astrophys. J.* in press (1996)

8. Brown, R.L. and Van den Bout, P.A., *Astrophys. J.*, **397**, L19–L22 (1992)

9. Solomon, P.M., Downes, D. and Radford, S.J.E., *Astrophys. J.* **398**, L29-L32 (1992)

10. Barvainis, R., Tacconi, L., Antonucci, R., Alloin, D., Coleman, P., *Nature*, **371**, 586-588 (1994)

11. Hu, E.M., McMahon, R.G. and Egami, E., *Astrophys. J. Lett.* **459**, L53-55 (1996)

12. Petitjean, P., Pécontal, E., Valls-Gabaud, D. and Charlot, S., *Nature* **380**, 411-413 (1996)

13. Djorgovski, S.G., in *Science with VLT*, Walsh, J.R. & Danziger, I.J. eds, (ESO, Springer, Berlin), 351 (1995)

14. Fontana, A., Cristiani, S., D'Odorico, S., Giallongo, E. and Savaglio, S., *MNRAS*, in press (1996)

15. Downes, D., Solomon, P.M. and Radford, S.J.E., *Astrophys. J.* **414**, L13-L16 (1993)

16. Barvainis, R., in: *Cold Gas at High Redshift*, M. Bremer, H. Rottgering, P. van der Werf & C. Carilli eds (Kluwer) (1996)

17. Barvainis, R., Antonucci, R., Hurt, T., Coleman, P. and Reuter, H.-P., *Astrophys. J.*, **451**, L9-L12 (1995)

18. Haehnelt, M.J., Rees, M.J., *MNRAS*, **263**, 168-178 (1993)

19. Wampler, E.J., Williger, G.M., Baldwin, J.A., Carswell, R.F., Hazard, C. and McMahon, R.G., *Astron. Astrophys.* in press (1996)

20. Magain, P. et al., *Nature*, **334**, 325-327 (1988)

21. Broadhurst, T. and Lehar, L., *Astrophys. J.*, **450**, L41-L44 (1995)

22. Eisenhardt, P.R., Arnus, L., Hogg, D.W., Soifer, B.T., Neugebauer, G. and Werner, M.W., *Astrophys. J.*, **461**, 72-83 (1996)

23. Downes, D., Solomon, P.M. and Radford, S.J.E. *Astrophys. J.* **453**, L65-L68 (1995)

24. Scoville, N.Z. et al., in : *Cold Gas at High Redshift*, M. Bremer, H. Rottgering, P. van der Werf & C. Carilli eds (Kluwer) (1996)

25. Storrie–Lombardi, L.J., McMahon, R.G., Irwin, M.J., Hazard, C., *Astrophys. J.* in press (1996)

26. Lu, L., Sargent, W.L.W., Womble, D.S., and Barlow, T.A., *Astrophys. J. Lett.*, **457**, L1-L4 (1996)

27. Djorgovski, S.G., Meylan, G., Klemola, A., Thompson, D.J., Weir, W.N., Swarup, G., Rao, A.P., Subrahmanyan, R., Smette, A., *MNRAS*, **257**, 240-244 (1992)

28. Franceschini, A. and Gratton, R., *MNRAS* submitted (1996)

29. Downes, D., Radford, S.J.E., Greve, A., Thum, C., Solomon, P.M. and Wink, J.E., *Astrophys. J.*, **398**, L25-L27 (1992)

33. Elston, R., Bechtold, J., Hill, G.J. and Jian G. *Astrophys. J. Lett.*, **456**, (1996)

Table 1 – Properties of BR1202–0725 and F10214+4724

	BR1202–0725		F10214+4724		Multiplier	Units
D_L	19		8.8		h^{-1}	Gpc
$S_{1.35mm}$	16		$7.7^{\dagger}$			mJy
z	4.69		2.29			
Line	CO(5–4)	CO(7–6)	CO(3–2)	CO(6–5)		
ν_{obs}	101.3	141.2	105.2	210.5		GHz
$S_{CO}\Delta V$	2.4	3.1	4.1^9	9.4^9		Jy km s^{-1}
L'$_{CO}$	1.5	1.0	2.6	1.5	$10^{10}A_G^{-1}h^{-2}$	K km s^{-1}pc^2
L$_{CO}$	9	16	3.5	16	$10^7A_G^{-1}h^{-2}$	L$_\odot$
M(H$_2$)	0.6		1.0		$10^{11}A_G^{-1}h^{-2}$	M$_\odot$
X(CO/1.3)	2.0		3.2		10^3	km s^{-1}

Symbols used : h = H$_o$/100 km s^{-1} Mpc^{-1}; A$_G$ is the (eventual) gravitational magnification for millimetre emission; D$_L$ is the luminosity distance (assuming q$_o$ = 0.5); ν_{obs} is the redshifted frequency; S$_{1.35mm}$ and S$_{CO}$ ΔV are the measured 1.35 mm flux density and

integrated CO flux respectively; L_{CO} and L'_{CO} are the CO line luminosities (eqs 1 and 3 of ref. 9); $M(H_2)$ is the nominal H_2 mass using $M(H_2) \propto L'_{CO}$; the ratio $M(H_2)/L'_{CO}$ is assumed 4 $M_\odot (km\ s^{-1}\ pc^2)^{-1}$ as in ref. 9 for F10214; the ratio $X = (1+z)^{1.5}\ S_{CO3mm}\ \Delta V/S_{1.35mm}$ should be approximately invariant for the same galaxy moved at different z (see eq. 3 of ref. 9 and eq. 1 of ref. 1). It is thus a good indication of the relative strength of the FIR/submm and CO emission. The difference between BR1202 and F10214 is hardly significant taking into account the calibration uncertainties and a small correction for the differences of frequency and line excitation. The total flux measured in the (4-3) line, 1.5 ± 0.3 $Jy\ km\ s^{-1}$, is in good agreement with the (5-4) line.

† $S_{1.25mm} = 9.6$ mJy from ref. 30, scaled to 1.35mm.

FIGURE CAPTIONS

Figure 1 – 1.35mm and 3mm maps.

For each band, two frequency setups were used to cover a total bandwidth of 0.9 GHz around the redshifted frequencies of the CO(5-4) (101 GHz) and CO(11-10) (223 GHz) lines. Coordinates are in the J2000.0 system.

Flux calibration was performed by using 3C273 and 3C279 which are monitored against planets by the IRAM staff; the flux densities were 13-18 Jy (3C273) and 13-16 Jy (3C279) at 223 GHz, with an estimated uncertainty about 10%. Linear polarisation of 3C279 has been accounted for in the calibration. The typical phase noise was 10 to 30 degrees at 223 GHz, and twice better at 3mm. For continuum data, the rms noise is 0.50 mJy/beam at 223 GHz, 0.22 mJy/beam at 101 GHz, 0.45 mJy/beam at 84 GHz.

Figure 1a – 1.35mm continuum image: obtained using natural weighting. The angular resolution is $2.0'' \times 1.3''$, at PA=12^0. Contour step is 1.0 mJy/beam or 2σ.

Superposed are the positions of the different visible features : Cross Q – QSO $\alpha(1950) =$ 12h 02m 49.26s $\pm$ 0.05s $\delta(1950)= -07^o$ 25' 51.0" $\pm$ 0.5" measured from the APM data.

Companion features with respect to the QSO[13] : Filled Triangle : Continuum feature – Filled Square : Lyα peak – Open Triangle : Second continuum feature.

The total integrated flux density is 16$\pm$ 2 mJy, and the deconvolved size of the elongated source around Q is $3.0'' \times 0.9'' \pm 0.7''$ at PA 120 ± 10^0.

Previous continuum measurements with the IRAM 30 m (full width at half maximum FWHM = 11") at 240 GHz are 10.5$\pm$1.5 mJy[1] and 12.3$\pm$2.3 mJy[6]. The measurements are done at different frequencies however. Given the very steep dust spectrum, the flux measured with the interferometer at 223 GHz (1.35mm) should correspond to a flux $\sim$

25 % smaller than at 240 GHz (1.25mm); but this should be approximately compensated by the possible small contribution of the CO(11-10) line. Altogether, given the calibration uncertainties of single measurements, especially with the 30m ($\sim$ 25%), the 30m and Bure determinations are consistent.

Figure 1b – 2.9mm continuum image – Contour spacings are 0.45 mJy/beam (2 σ). Contribution from CO line emission over velocities between –170 and +360 km/s has been avoided. The angular resolution is $5.0'' \times 2.5''$ at PA = 20^0.

Figure 1c – 3.7mm continuum image – Contour spacings are 0.45 mJy/beam (1 σ). Contribution from CO line emission over velocities between –160 and +280 km/s has been avoided. The angular resolution is $6.4'' \times 2.7''$ at PA = 164^0.

Figure 1d – Map of the CO(5–4) line integrated flux within the velocity range + 7 km/s – +360 km/s, peaking towards the QSO. Contour spacings are 2 σ (0.32 Jy/beam.km/s, corresponding to 0.9 mJy/beam for continuum emission). Same angular resolution has Fig. 1b.
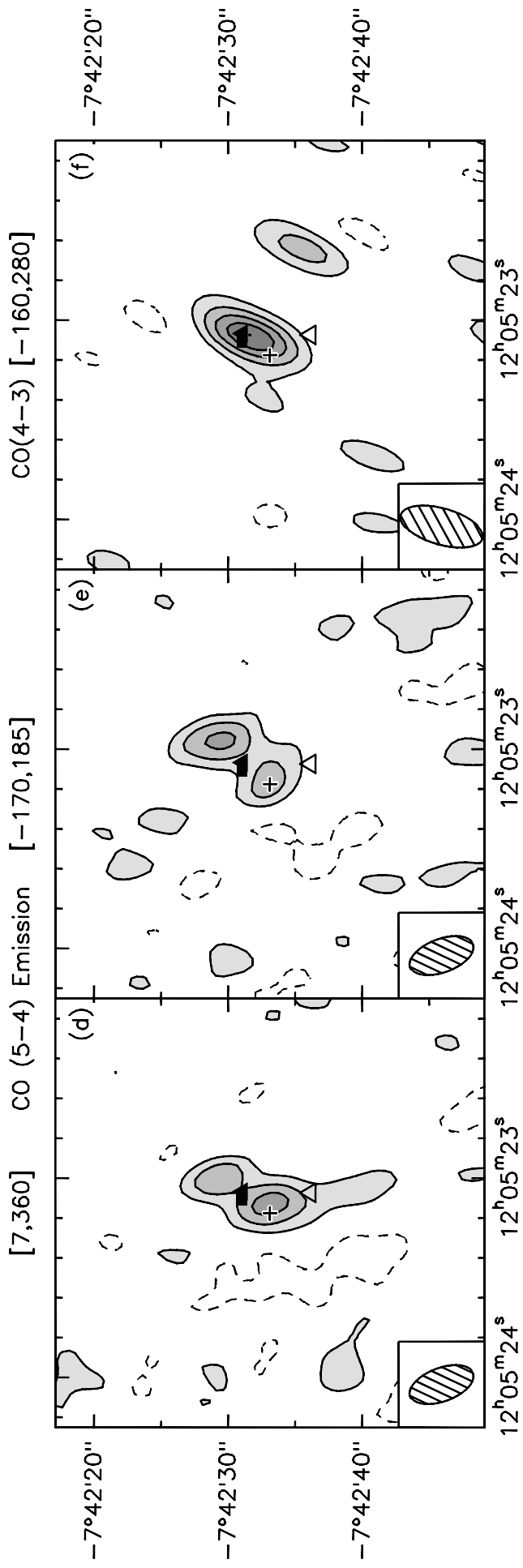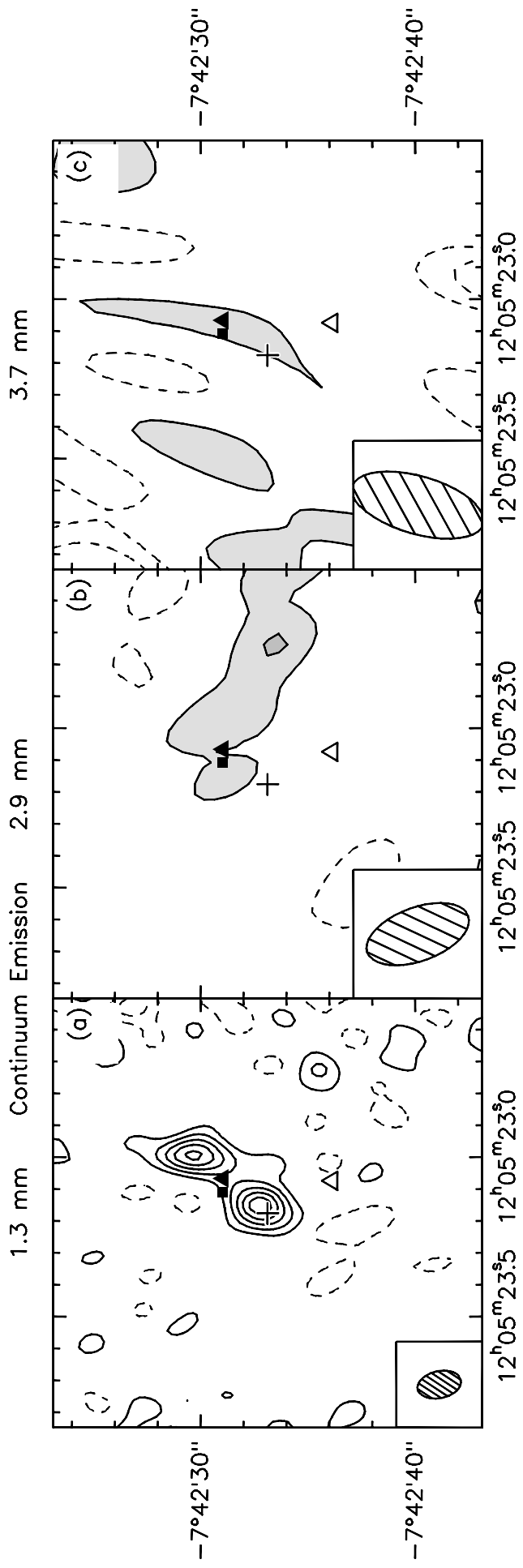
Figure 1e – Same as Fig. 1c for the velocity range – 170 km/s – + 185 km/s, peaking towards the NW component.

Figure 1f – Map of the CO(4–3) line integrated flux within the velocity range –160 km/s – +280 km/s. Contour spacings are 2 σ (0.26 Jy/beam.km/s, corresponding to 0.6 mJy/beam for continuum emission). Same angular resolution has Fig. 1c. The unfavorable beamshape precludes separation of the two components.

Figure 2 – Spectra of the CO(5-4) line emission superimposed to the 1.35mm continuum image. For each spectrum, the curve is the best fit gaussian profile with no baseline

removed.

Insert – Spectrum of CO(7–6) line observed with the IRAM 30m telescope. The velocity and redshift scales are identical for the CO(5-4) and CO(7-6) spectra.

1.3 mm   Continuum Emission   2.9 mm   3.7 mm

(a) (b) (c)

CO (5–4) Emission [–170,185] CO(4–3) [–160,280]

[7,360]

(d) (e) (f)

CO (5-4) & (7-6) towards BR1202-0725

Declination (J2000.0)

Right Ascension (J2000.0)

Redshift

CO(7-6)

Flux (mJy)

Velocity (km/s)